The American Journal of Pathology, Vol. 170, No. 5, May 2007

DOI: 10.2353/ajpath.2007.061111

Growth Factors, Cytokines, Cell Cycle Molecules

Epigenetic Silencing through DNA and Histone Methylation of Fibroblast Growth Factor Receptor 2 in Neoplastic Pituitary Cells

Xuegong Zhu,*† Katie Lee,†‡ Sylvia L. Asa,†‡ and Shereen Ezzat*†

From the Department of Medicine, Mount Sinai Hospital and University of Toronto; The Ontario Cancer Institute†; and the Department of Pathology,‡ University Health Network and University of Toronto, Toronto, Ontario, Canada*

Four members of the fibroblast growth factor receptor (FGFR) family of tyrosine kinases transduce signals of a diverse group of more than 23 fibroblast growth factor (FGF) ligands. Each prototypic receptor is composed of three immunoglobulin-like extracellular domains, two of which are involved in ligand binding. Alternative RNA splicing of one of two exons results in two different forms of the second half of the third immunoglobulin-like domain, the IIIb or IIIc isoforms. The contribution of each receptor and their isoforms in tumorigenesis remains unknown. In the pituitary, FGFR2 is expressed primarily as the IIIb isoform in normal adenohypophysial cells. In contrast, FGFR2 is significantly down-regulated in mouse corticotroph AtT20 tumor cells where the 5′ promoter is methylated. Treatment of AtT20 cells with 5′-azacytidine resulted in FGFR2 re-expression, mainly as the FGFR2-IIIb isoform. Chromatin immunoprecipitation revealed evidence of histone methylation, but not of deacetylation, in the silencing of FGFR2 in AtT20 cells. Exposure of these cells to the cognate FGFR2-IIIb ligand FGF-7 resulted in diminished Rb phosphorylation and accumulation of p21 and p27, indicating diminished cell cycle progression. Examination of primary human pituitary adenomas revealed FGFR2 down-regulation in 52% (11 of 21) of samples and FGFR2 promoter DNA methylation in 45% (10 of 22) of samples. These data highlight the contribution from DNA and histone methylation as epigenetic mechanisms responsible for FGFR2 silencing in pituitary neoplasia. ***(Am J Pathol 2007, 170:1618–1628; DOI: 10.2353/ajpath.2007.061111)***

Pituitary tumors make up nearly 10% of all surgically excised intracranial neoplasms. They typically cause morbidity through invasive growth into surrounding brain and bony structures. Pituitary tumorigenesis rarely involves intragenic mutations of classical oncogenes or tumor suppressor genes.[1,2] Instead, evidence suggests that growth signals implicated in pituitary development may be relevant to the tumorigenic processes in this gland, particularly involving protein members of the bone morphogenic protein, Wnt, and fibroblast growth factor (FGF) families.[3,4]

There are 23 members of the FGF family of ligands, and their receptors are encoded by four genes that give rise to multiple isoforms of secreted and membrane-bound receptors derived by alternative initiation, alternative splicing, and C-terminal truncations.[5] The FGF receptor 2 (FGFR2) gene is alternatively spliced to generate FGFR2-IIIb, an isoform containing the second half of the third Ig-like domain encoded by exon 7 (also referred to as KGFR or Ksam-IIC1) that binds FGF1, FGF3, FGF7, and FGF10 with high affinity.[6,7] In contrast, the FGFR2-IIIc isoform encoded using exon 8 (also referred to as Bek), binds FGF1 and FGF2 but not FGF7 or FGF10.[8,9] FGFR2-IIIb expression is tightly restricted to epithelial cells, whereas FGFR2-IIIc is typically expressed in mesenchymal cells.[10]

FGF signaling is critical in pituitary development.[5] In particular, deletion of the FGF10 ligand or its receptor, the FGFR2-IIIb isoform, leads to failure of pituitary development.[11] Mid-gestational expression of a soluble dominant-negative FGFR results in severe pituitary dysgenesis.[12] Likewise, multiple lines of evidence have supported the involvement of members of the FGF/FGFR family in pituitary tumorigenesis. Selected FGF ligands are overexpressed in pituitary tumors.[13] Systemic estrogen-induced pituitary tumorigenesis in Wistar rats is accompa-

Supported by the Canadian Institutes of Health Research (grant MT-14404) and by Toronto Medical Laboratories.

Accepted for publication February 6, 2007.

Address reprint requests to Dr. Sylvia L. Asa, Ontario Cancer Institute, 610 University Ave. 8-209, Toronto, ON, Canada M5G 2M9. E-mail: sylvia.asa@uhn.on.ca.

nied by enhanced FGF-2 expression.[14] Moreover, the human endogenous FGF antisense gene is expressed in the normal pituitary, where it restricts cell proliferation, and its expression is reduced in pituitary tumors.[15]

We have previously demonstrated altered expression of several members of the FGFR family in pituitary tumors.[16] In particular, we found that FGFR4 is N-terminally truncated to yield a pituitary tumor-derived FGFR4[16,17] as a result of alternative transcription initiation using a cryptic promoter.[18,19] In contrast to wild-type FGFR4, pituitary tumor-derived FGFR4 does not associate with neural cell adhesion molecule and interferes with N-cadherin to impede cell adhesion.[20]

We have previously observed that FGFR2 is expressed by the normal pituitary, but its expression is diminished in human pituitary tumors.[16] FGFR2 down-regulation has been previously described with tumor progression in astrocytomas, bladder and prostatic carcinomas, and thyroid carcinomas.[21–25] Forced FGFR2-IIIb expression significantly retards thyroid tumor progression while enhancing apoptosis.[25] Given the recognized role for FGFR2 in the development of the anterior pituitary gland[1] and the common theme of epigenetic silencing in human pituitary tumorigenesis,[26] we examined potential mechanisms through DNA as well as histone modifications by which this gene could be silenced in neoplastic pituitary cells.

Materials and Methods

Cell Culture Conditions and Human Pituitary Tumor Specimens

Mouse pituitary corticotroph AtT20 cells were obtained from the American Type Culture Collection (Rockville, MD) and grown in Ham F-10 medium supplemented with 15% horse serum and 2.5% fetal calf serum (all from Sigma, St. Louis, MO) with 2 mmol/L glutamine, 100 IU/ml penicillin, and 100 μg/ml streptomycin (37°C, 95% humidity, 5% CO_2 atmosphere incubation).

Twelve normal human pituitary specimens with no morphological abnormalities and 36 primary human pituitary adenomas were obtained at the time of surgery after informed consent and institutional review. The pathology of pituitary adenomas was examined using immunohistochemistry for all cases, and tumors were classified histologically according to the accepted Armed Forces Institute of Pathology and World Health Organization criteria;[27,28] the details are summarized in Table 1.

5-Aza-2′-Deoxycytidine and Trichostain-A Treatments

AtT20 cells were plated at 1×10^6 cells/10-cm dish and allowed to attach for 24 hours. For assessment of the impact of DNA methylation, cells were treated with the DNA methyltransferase inhibitor 5-Aza-2′-deoxycytidine (5-Aza-dC) (Sigma) at concentrations of 5 or 10 μmol/L for 5 days. These doses were based on preliminary dose-response analyses in AtT20 cells. At 24-hour intervals, new medium containing freshly prepared drug was added. For assessment of chromatin histone acetylation, cells were treated with 0.3 and 0.6 μmol/L histone deacetylase inhibitor trichostatin-A (TSA) (Sigma) for 24 hours. Each experiment was independently performed with three separate dishes in at least three independent experiments.

Western Blotting

Cells were lysed with radioimmunoprecipitation assay buffer [1% NP-40, 0.5% sodium deoxycholate, 0.1% sodium dodecyl sulfate (SDS), 100 μg/ml phenylmethylsulfonyl fluoride, aprotinin, and sodium orthovanadate in PBS]. Total cell lysates were quantified by the Bio-Rad (Hercules, CA) method. Fifty micrograms of whole lysates was separated on 10% SDS denaturing polyacrylamide gels and transferred onto a nylon membrane (Millipore, Bedford, MA) at 100 V for 1.5 hours at room temperature. Blots were incubated with a rabbit polyclonal IgG antibody that recognizes the C-terminal fragment of FGFR2 (c-17; Santa Cruz Biotechnology) or FGFR1 (C-15; Santa Cruz Biotechnology), both at 1:2000 dilution, in PBS-5% nonfat milk with 0.1% Tween at 4°C overnight, followed by washing with PBS-Tween 20 four times of 10 minutes each at room temperature, then incubated with peroxidase-conjugated goat anti-rabbit IgG horseradish peroxidase (1:2000) for 1 hour at room temperature with agitation. Protein bands were visualized using chemiluminescence (Amersham, Oakville, ON, Canada). Experiments were performed on three independent occasions with product intensities quantified by scanning densitometry (Quantity One Software; Bio-Rad).

Immunocytochemistry

FGFR2 expression in human pituitary tumors and AtT20 pituitary cell pellets was examined by immunocytochemistry on 4-μm sections of tissue. Briefly, sections were treated with 2% hydrogen peroxide to quench endogenous peroxide for 30 minutes and exposed to 5 μg/ml proteinase K for 15 minutes at room temperature. The sections were washed extensively and exposed to equilibration buffer for 10 minutes. Each slide was then incubated with anti-FGFR2 antibody (polyclonal antibody C-17; Santa Cruz Biotechnology) at 4°C overnight. The reaction was visualized with the avidin-biotin method and 3,3′-diaminobenzidine.

Microdissection and DNA Extraction

After immunocytochemistry, slides were visualized under an inverted microscope and microdissected using a 26-gauge needle. FGFR2-positive and -negative areas were microdissected. Microdissected tissue was digested overnight at 50°C in a buffer containing 50 mmol/L Tris-HCl, pH 8.0, 0.1 mmol/L ethylenediamine tetraacetic acid, pH 8.0, 0.1 mmol/L NaCl, 1% SDS, and 200 μg/ml proteinase K, followed by phenol/chloroform extraction and ethanol precipitation. DNA was stored at −20°C for polymerase chain reaction (PCR) amplification.

Table 1. List of Primary Human Pituitary Samples

Case number	Sex	Pathologic diagnosis	mRNA expression	Isoform content	DNA methylation
mRNA analyses					
1	M	Normal	+	IIIb	
2	F	Normal	+	IIIb/IIIc	
3	F	Normal	+	IIIb/IIIc	
4	M	Normal	±		
5	M	Normal	+		
6	F	Normal	+	IIIb/IIIc	
13	F	Corticotroph adenoma	−		
14	M	Lactotroph adenoma (sparsely granulated)	−		
15	F	Silent subtype 3 adenoma	−		
16	M	Mixed lactotroph-somatotroph adenoma	+	IIIb/IIIc	
17	M	Somatotroph adenoma (densely granulated)	−		
18	F	Lactotroph adenoma	−		
19	F	Lactotroph adenoma	−		
20	M	Oncocytic adenoma	+		
21	F	Gonadotroph adenoma	+		
22	F	Somatotroph adenoma (sparsely granulated)	+	IIIb	
23	M	Somatotroph adenoma (densely granulated)	−		
24	F	Somatotroph adenoma (densely granulated)	±		
25	F	Corticotroph adenoma	+		
26	M	Somatotroph adenoma (sparsely granulated)	−		
DNA analyses					
7	F	Normal			−
8	M	Normal			−
9	M	Normal			−
10	F	Normal			+
11	M	Normal			−
12	F	Normal			−
27	F	Acidophil stem cell adenoma			+
28	M	Gonadotroph adenoma			+
29	F	Gonadotroph adenoma			−
30	F	Lactotroph adenoma (sparsely granulated)			+
31	M	Lactotroph adenoma (sparsely granulated)			−
32	F	Somatotroph adenoma (sparsely granulated)			+
33	M	Lactotroph adenoma (sparsely granulated)			±
34	M	Somatotroph adenoma (sparsely granulated)			−
35	M	Gonadotroph adenoma			+
36	M	Somatotroph adenoma (densely granulated)			+
37	F	Lactotroph adenoma			−
38	F	Corticotroph adenoma			−
39	F	Corticotroph adenoma			−
40	M	Lactotroph adenoma (sparsely granulated)			+
41	M	Mixed lactotroph-somatotroph adenoma			−
mRNA and DNA analyses					
42	M	Lactotroph adenoma (sparsely granulated)	−		+
43	M	Oncocytic adenoma	−		+
44	M	Somatotroph adenoma (sparsely granulated)	+	IIIb/IIIc	−
45	M	Gonadotroph adenoma	±		±
46	M	Oncocytic adenoma	−		+
47	F	Oncocytic adenoma	+		−
48	M	Gonadotroph adenoma	+	IIIb/IIIc	−

M, male; F, female; +, strong; −, negative; ±, intermediate.

RNA Extraction and Isoform Examination

Total RNA was isolated from AtT20 cells treated with different concentrations of 5-Aza-dC or TSA using TriZol reagents (Invitrogen Corp., Carlsbad, CA) according to the manufacturer's instructions. Approximately 1.0 μg of total RNA from each sample was reverse transcribed in a 20-μl volume using the TaqMan reverse transcription reagents kit (Applied Biosystems, Foster City, CA). The reaction mixture was incubated at 25°C for 10 minutes, 42°C for 30 minutes, and 95°C for 5 minutes. The synthesized cDNA was used for PCR amplification or stored at −20°C for further analysis. Both mouse and human reverse transcriptase-PCR (RT-PCR) primers were designed to span exons 6 to 9 of FGFR2, the region that contains exon 7 (encoding the FGFR2-IIIb isoform) and exon 8 (encoding the FGFR2-IIIc isoform) (Table 2). PCR was performed for 10 minutes at 95°C followed by 35 cycles of 30 seconds at 95°C, 30 seconds at annealing temperature, and 30 seconds at 72°C, followed by a 10-minute extension at 72°C in a reaction mixture containing 1.5 mmol/L $MgCl_2$, 0.2 mmol/L dNTP, 0.2 mmol/L of each primer, and 0.375 U of Ampli*Taq* Gold polymer-

Table 2. List of Primers and PCR Conditions

Primer	Forward	Reverse	Tm (°C)	Product size (bp)
RT-PCR				
Mouse RT-exon (6 to 9)	5′-GGATCAAGCACGTGGAAAAGAAC-3′	5′-ACCATGCAGGCGATTAAGAAGAC-3′	58	307
Mouse GAPDH	5′-ATCACTGCCACCCAGAAGACT-3′	5′-CATGCCAGTGAGCTTCCCGTT-3′	56	152
Human RT-exon (6 to 9)	5′-GGATCAAGCACGTGGAAAAGAAC-3′	5′-GGCGATTAAGAAGACCCCTATGC-3′	60	310
Human PGK	5′-GCTGACAAGTTTGATGAGAAT-3′	5′-AGGACTTTACCTTCCAGGAGC-3′	58	338
Bisulfite sequencing				
Mouse (outer)	5′-TTATTGTGTATTAAAGTTGGTTAGGAATTG-3′	5′-AACCAAAAACACACAAACAACCCC-3′	56	
Mouse (inner)	5′-TAAAGTTGGTTAGGAATTGGGGTAGTG-3′	5′-AACCAAAAACACACAAACAACCCC-3′	56	399
Human	5′-GAGTAAAGTTTGGTGGAGGTAA-3′	5′-CAAAAAAATAATCCTTAAATCTTC-3′	51	165
MSP				
Mouse methylation	5′-CGAGAGGTTATTTGTGTATTTTTGCG-3′	5′-GAACCGTTTCCTAAACGACGACG-3′	56	166
Mouse unmethylation	5′-TGAGAGGTTATTTGTGTATTTTTGTGG-3′	5′-AAACCATTTCCTAAACAACAACACC-3′	56	166
Human methylation	5′-GTAGTTTGGGGTACGCGTGAAGTTC-3′	5′-CCCGCGTAAATCGAAATAAAAAAAA-CG-3′	59	128
Human unmethylation	5′-AGTTTGGGGTATGTGTGAAGTTTGG-3′	5′-CCCCACATAAATCAAAATAAAAAAA-ACAAC-3′	57	127
Chromatin immunoprecipitation				
Mouse	5′-ACCAAAGCTGGCTAGGAACTGG-3′	5′-CTAGCAGCCGCAAAGAGACACC-3′	59	140

GAPDH, glyceraldehyde-3-phosphate dehydrogenase; Tm, annealing temperature; PGK, phosphoglycerate kinase.

ase (Applied Biosystems). PCR products were separated on 2.0% agarose gels and visualized with ethidium staining.

Restriction Digestion

RT-PCR products from AtT20 cells and from primary human pituitary samples were purified using Ultrafree-MC centrifugal filter units (Millipore). Ten micrograms of purified PCR products was incubated in a 15-μl volume reaction with 5 U of restriction endonuclease *Ava*I or *Eco*RV (Roche, Penzberg, Germany) overnight at 37°C. Restriction digestion products were separated on 12% SDS denaturing polyacrylamide gels, followed by a 5-minute immersion in ethidium bromide for UV exposure. Experiments were performed on three independent occasions, after which product intensities were quantified by scanning densitometry (Quantity One Software; Bio-Rad).

Bisulfite Sequencing and Methylation-Specific PCR

One microgram of genomic DNA was bisulfite-modified according to the manufacturer's protocol (Chemicon International, Temecula, CA) diluted in a 25-μl volume. One microliter of modified DNA was used for methylation-specific PCR (MSP) and bisulfite sequencing. Primer location, sequence, and PCR conditions are indicated in Table 2. Two rounds of PCR reactions were performed for bisulfite sequencing, both for 10 minutes at 95°C followed by 40 cycles of 30 seconds at 95°C, 45 seconds at 56°C, and 45 seconds at 72°C, followed by a 10 minutes extension at 72°C in a reaction mixture containing 1.5 mmol/L $MgCl_2$, 0.2 mmol/L dNTP, 0.2 mmol/L of each primer, and 0.25 U/10 μl of Ampli*Taq* Gold polymerase (Applied Biosystems). Final PCR products were cut from 1.5% agarose gels, extracted, and cloned using the TA cloning system (Invitrogen) for automated sequencing. At least 10 positive clones from each sample were sequenced.

For MSP, both mouse and human unmethylated reactions were performed as for bisulfite sequencing reactions but using different annealing temperatures (Table 2) and 5.0 mmol/L $MgCl_2$. All reactions were performed on at least three independent occasions.

Chromatin Immunoprecipitation Assays

The chromatin immunoprecipitation assay was performed in accordance with the manufacturer's recommendations (UBI, Lake Placid, NY) and as previously described.[18] In brief, histone was cross-linked to DNA by the direct addition of 37% formaldehyde, and cells were washed with ice-cold PBS containing protease inhibitors before lysis. The lysates were sonicated to shear DNA lengths between 200 and 1000 bp. After centrifugation, cell suspensions were further diluted, and 20 μl of lysate from each sample was used to monitor the amount of DNA present (input DNA) for PCR detection. The rest of the lysate was cleared with salmon sperm DNA/protein G-agarose beads. Immunoprecipitation was performed using anti-methyl-histone 3 (Lys9), anti-acetyl-histone H3 (AcH3), and anti-acetyl-histone H4 antibody (all from UBI) overnight at 4°C with agitation. Negative controls included omission of antibody or use of an anti-IgG antibody. For PCR analysis, the histone-DNA cross-links of eluates were reversed at 65°C, the immunocomplexes were digested with proteinase K for 1 hour at 50°C, and DNA was finally purified by phenol extraction and used for PCR amplification. PCR primers and conditions are shown in Table 2. PCR reactions were performed in a volume of 15 μl containing 1.5 mmol/L $MgCl_2$, 0.2 mmol/L dNTP, 0.2 mmol/L of each primer, and 0.375 U of Ampli-

Taq Gold polymerase (Applied Biosystems). Experiments were performed on three independent occasions and quantified by scanning densitometry (Quantity One Software; Bio-Rad).

Impact of FGFR2 on Pituitary Cell Cycle Progression

We used the FGF-7 ligand to examine the impact of FGFR2 activation on pituitary cell cycle progression. This FGF was chosen on the basis of its selective binding to FGFR2.[7] One million AtT20 cells were treated with FGF-7 (25 ng/ml) or vehicle (as control) for 24 hours in the presence of heparin (10 U/ml). Cells were subsequently lysed and examined by Western blotting for markers of cell cycle progression. These included Rb phosphorylation (phospho-Rb Ser780, polyclonal 1:1000; Cell Signaling Technology, Beverly, MA), the cyclin-dependent kinase inhibitors p21 (polyclonal 1:500; BD Biosciences, Mississauga, ON, Canada) and p27 (monoclonal 1:1000; Transduction Laboratories, Lexington, KY), and actin (monoclonal 1:500; Sigma) as a loading control.

Results

FGFR2 Expression in AtT20 Pituitary Tumor Cells Is Up-Regulated by Methylation Inhibition

We used the well-established mouse pituitary AtT20 corticotroph line as our cellular model. This tumorous cell line revealed faintly detectable FGFR2 protein expression by Western blotting (Figure 1a), in contrast to the strong expression in normal mouse pituitary. Treatment of AtT20 cells with the methylation inhibitor 5-Aza-dC resulted in a robust 15-fold increase in FGFR2 protein levels (Figure 1b). To examine the possibility that histone deacetylation might also be a contributory factor to FGFR2 down-regulation, we examined the impact of the histone deacetylase inhibitor TSA treatment. In contrast to 5-Aza-dC, TSA treatment resulted in a more modest fivefold enhancement of FGFR2 expression (Figure 1b). Immunocytochemical detection of corresponding cell pellets confirmed enhanced FGFR2 membranous staining after both treatments (Figure 1c). Neither pharmacological treatment, however, resulted in any detectable impact on FGFR1 expression (data not shown).

Alternative splicing of the third Ig-like extracellular domain of FGFR2 results in two major transcripts referred to as FGFR2-IIIb and FGFR2-IIIc due to inclusion of exon 7 or 8, respectively (Figure 2a). These two isoforms display distinct FGF binding with differing functional properties.[6] Unique restriction sites in exons 7 (*Ava*I) and 8 (*Eco*RV) permitted isoform characterization of PCR products (Figure 2a). Figure 2b demonstrates that the effects of 5-Aza-dC or TSA treatment can be identified at the mRNA level. This closely approximates the level of expression in the normal mouse pituitary (Figure 2b). Moreover, restriction digestion demonstrates that the IIIb isoform accounts for a greater proportion of FGFR2 mRNA expression after

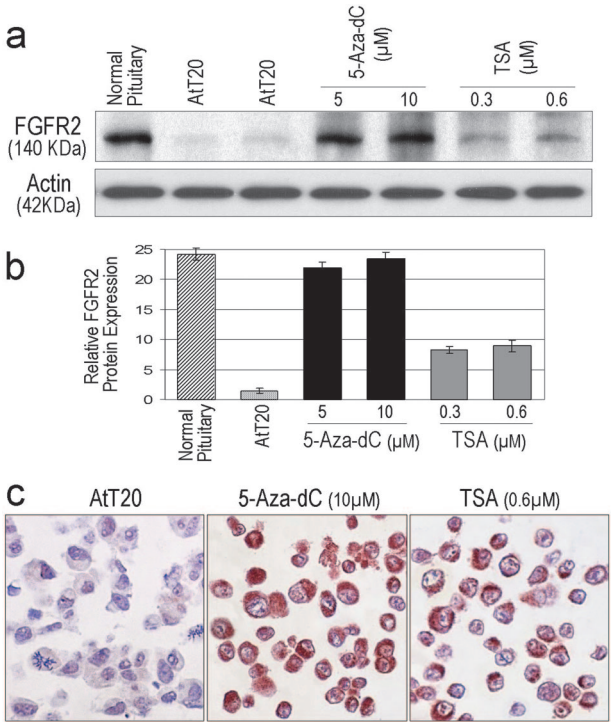

Figure 1. FGFR2 expression before and after treatment with 5-Aza-dC and TSA in mouse pituitary corticotroph AtT20 cells. **a:** Western blotting detects increased FGFR2 protein expression in normal mouse pituitary with markedly reduced expression in AtT20 cells. Re-expression of FGFR2 is noted after treatment with 5 or 10 μmol/L 5-Aza-dC and to a lesser extent after TSA treatment as detailed in Materials and Methods. **b:** FGFR2 protein concentrations were quantified by Quantity One Software (Bio-Rad). Displayed graphically are the means of FGFR2 protein concentrations ± SEM from three replicates for each treatment. **c:** Corresponding cell pellets as shown in **b** were also examined by immunocytochemistry for FGFR2 detection and localization.

inhibition of methylation (Figure 2c). This greater contribution of FGFR2-IIIb isoform expression was comparable with that noted in normal mouse pituitary cells (Figure 2c, left).

DNA and Histone Methylation Contribute to Pituitary Tumor FGFR2 Down-Regulation

The mouse FGFR2 promoter region from −665 to 470 encompassing the 5′-untranslated region and exon 1 contains two large CpG islands (−239 to 245 and 263 to 414) (Figure 3a). Sequencing data from representative clones are shown in Figure 3c. The corresponding 53 potential methylation sites were reversed after 5-Aza-dc treatment (Figure 3, b and c). Likewise, MSP demonstrated significant DNA methylation in untreated AtT20 cells (Figure 3d). DNA demethylation was specifically noted after 5-Aza-dC treatment but not after TSA treatment.

To determine the potential role of histone modifications in FGFR2 down-regulation in AtT20 cells, we performed chromatin immunoprecipitation assays amplifying the corresponding region using methylation-specific (MeH3) and acetylation-specific (AcH3 and AcH4) antibodies (Figure 3e). This approach identified a significant impact of 5-Aza-dC treatment on histone methylation. As antici-

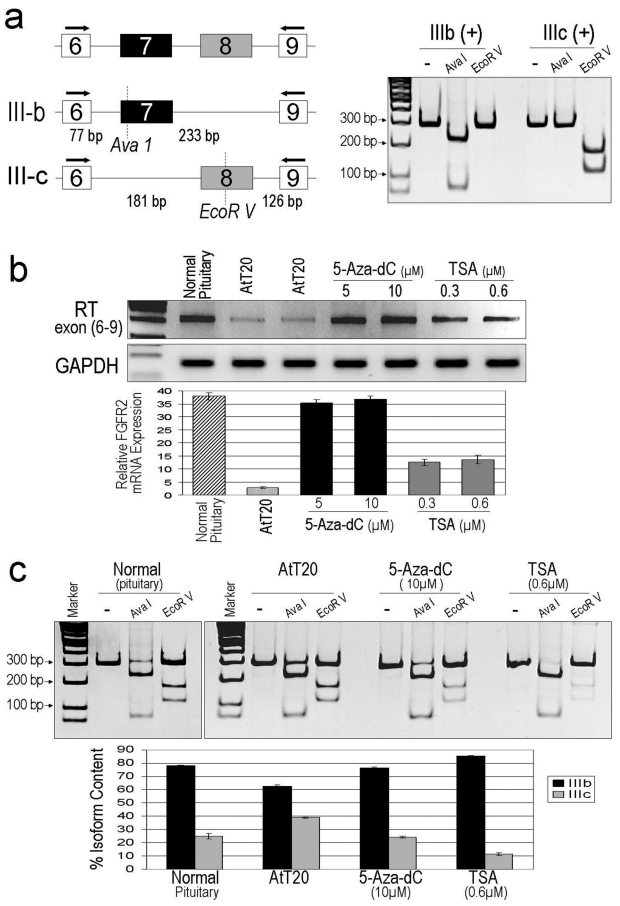

Figure 2. FGFR2 mRNA expression analysis in AtT20 cells after treatment with 5-Aza-dC and TSA. **a:** Alternative splicing of the FGFR2 gene to include exon 7 or 8 results in isoform IIIb or IIIc, respectively. Primers (denoted by **arrows**) used in RT-PCR to detect FGFR2 expression changes at the mRNA level target the common regions, exons 6 and 9, allowing amplification of both IIIb and IIIc isoforms. Subsequent restriction digestion of cDNA controls (right) allows determination of isoform expression. *Ava*I recognizes the specific sequence CTCGGG found in the IIIb isoform to yield two fragments (77 and 233 bp) on digestion. *Eco*RV recognizes the specific sequence GATATC found in the IIIc isoform to yield two fragments (181 and 126 bp) on digestion. **b:** RT-PCR analysis amplifying exons 6 to 9. Note down-regulation of FGFR2 in AtT20 cells compared with normal mouse pituitary. Note impact of 5-Aza-dC and of TSA on enhanced mRNA expression. **c:** Restriction endonuclease digestion of equalized PCR products (10 μg/lane) from normal mouse pituitary gland and from AtT20 cells as indicated were visualized on 12% SDS denaturing polyacrylamide gel. −, no enzyme treatment. Concentrations of digestion products measured by Quantity One Software represent content of the IIIb and IIIc isoforms in normal mouse pituitary and in AtT20 cells as controls or after treatment with 5-Aza-dc or TSA. Displayed graphically are the means of digestion product isoform content ± SEM from three replicates for each treatment performed in three separate experiments.

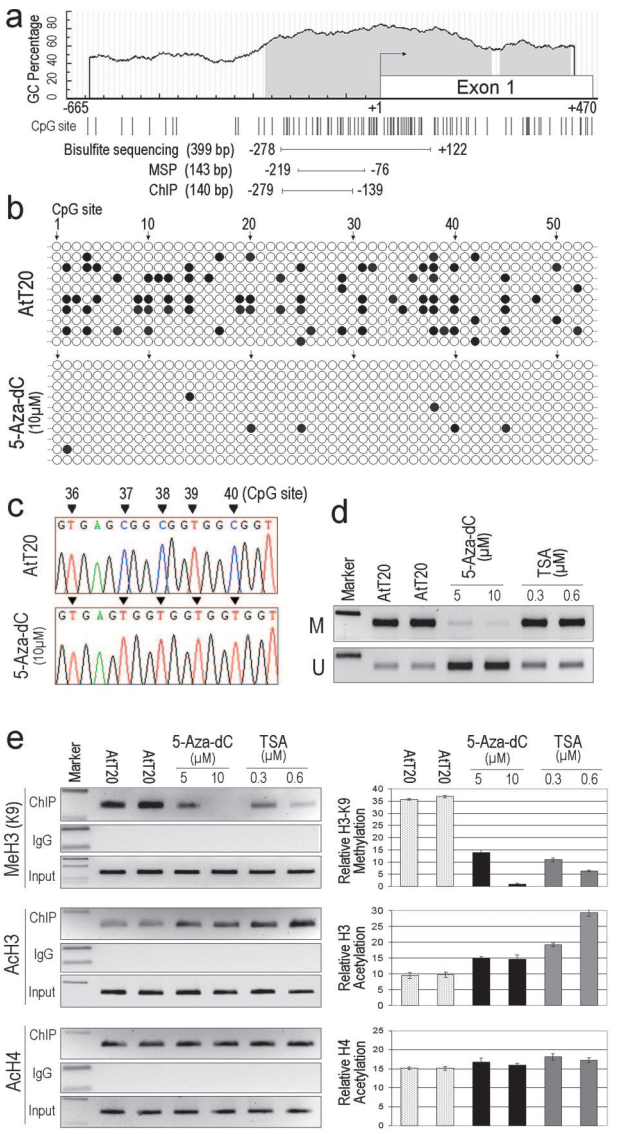

Figure 3. DNA methylation and chromatin immunoprecipitation analyses in AtT20 cells after 5-Aza-dC and TSA treatment. **a:** The mouse FGFR2 promoter region from −665 to 470 encompassing the 5′-untranslated region and exon 1 contains two large CpG islands (−239 to 245 and 263 to 414). Aberrant CG sites are denoted by vertical bars below the graph. Bisulfite sequencing and MSP examined the methylation status of the gene promoter. Chromatin immunoprecipitation analysis examined histone modification effects on gene inactivation. Sequence numbering follows GenBank accession NC 000073. **b:** Bisulfite sequencing was performed from −278 to 122, which includes 53 CpG dinucleotide sites. Results from bisulfite sequencing reveal partial methylation in control AtT20 cells, which was reversed by 5-Aza-dC treatment. Individual methylated CpG sites are indicated by closed circles. Each row represents an individual clone. **c:** A representative clone of the bisulfite-derived sequence is shown here in untreated cells (AtT20) and after 5-Aza-dC treatment. **d:** MSP analysis using methylated specific (M) and unmethylated-specific (U) primers as depicted in **a** are shown. **e:** Chromatin immunoprecipitation analysis covering the region indicated in **a** using three different antibodies, anti-methyl-histone H3-Lys9 (MeH3-K9), anti-acetyl-histone H3 (AcH3), and anti-acetyl-histone H4 (AcH4), performed on untreated and 5-Aza-dc- and TSA-treated AtT20 cells. Nonspecific antibody (IgG) was used as a negative control. Input lanes reflect PCR reaction products without prior immunoprecipitation. Displayed graphically to the right are the mean ± SEM from three replicate experiments.

pated, TSA treatment resulted in enhanced histone 3 acetylation. Interestingly, TSA treatment also inhibited histone methylation, further emphasizing the balance between the two histone modifications in FGFR2 control. Minimal impact was noted by either pharmacological treatment on histone 4 acetylation.

FGF-7 Treatment of Pituitary Cells Impedes Cell Cycle Progression

To determine a functional impact of FGFR2 on pituitary cells, we examined the effect of FGF-7 on AtT20 cell cycle progression. We chose FGF-7 based on its ability to selectively bind and activate FGFR2-IIIb.[7] Exposure of AtT20 cells to FGF-7 resulted in diminished cell cycle progression. This was evidenced by diminished Rb phos-

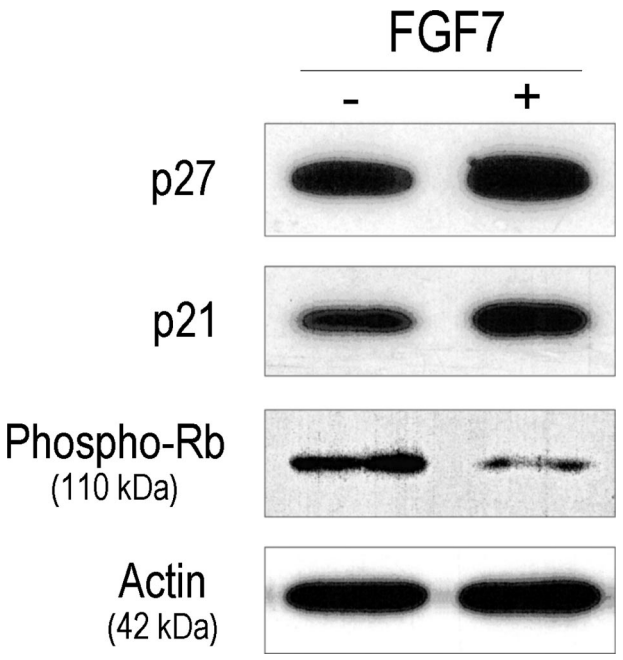

Figure 4. FGF-7 impedes pituitary AtT20 cell cycle progression. Twenty-four hours after serum deprivation, cells were exposed to the FGFR2-IIIb ligand FGF-7 in the presence of heparin for 24 hours. Cell lysates were resolved by Western blotting for detection of Rb phosphorylation (phospho-Rb) and accumulation of the cyclin-dependent kinase inhibitors (CDKIs) p21 and p27, reflecting cell cycle progression.

phorylation accompanied by corresponding accumulation of the cyclin-dependent kinase inhibitors p21 and p27 (Figure 4).

FGFR2 Is Down-Regulated in Primary Human Pituitary Tumors

To corroborate the implications of our findings on FGFR2 methylation and down-regulation in mouse pituitary cells, we examined primary human pituitary surgical specimens. RT-PCR analysis spanning exons 6 to 9 was performed on RNA from 27 clinical samples including six samples that were morphologically free of disease and 21 human pituitary adenoma samples (Table 1). As previously described,[16] normal human pituitary tissue demonstrated readily detectable FGFR2 mRNA expression (Figure 5a). In contrast, mRNA expression was significantly down-regulated in 11 of 21 (52.4%) pituitary tumor samples. Restriction endonuclease digestion identified the presence of the IIIb and, to a lesser extent, IIIc isoforms in normal human pituitary specimens (Figure 5b). Similar examination of FGFR2-positive primary human pituitary tumors showed predominantly FGFR2-IIIb expression in some (Figure 5c, tumor 22) with a mixed pattern of FGFR2-IIIb and IIIc isoforms in others (Figure 5c, tumors 16, 44, and 48).

FGFR2 Is Hypermethylated in Human Pituitary Tumors

The human FGFR2 promoter region from −596 to 441 encompassing the 5′-untranslated region and exon 1

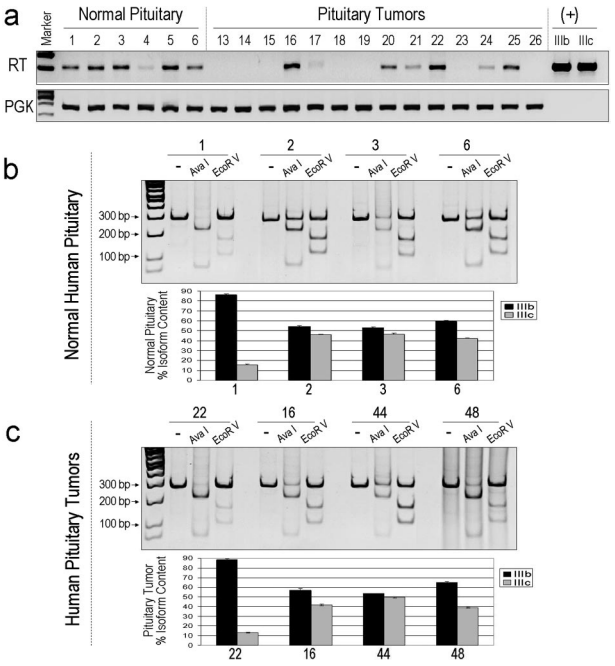

Figure 5. FGFR2 is down-regulated in human pituitary tumors. **a:** RT-PCR amplification of FGFR2 was performed on primary human pituitary samples including six normal pituitary specimens and 14 pituitary tumors. Restriction endonuclease digestion of equalized amounts of PCR products (10 μg) from **a** were visualized on 12% SDS denaturing polyacrylamide gel. Lanes are marked by numbers that represent individual samples of normal pituitary or pituitary tumor (see Table 1). Refer to Figure 2a for details on *Ava*I and *Eco*RV. −, no enzyme treatment. Concentrations of digestion products measured by densitometry are representative of the FGFR2-IIIb and IIIc isoform content as a fraction of the total in normal (**b**) and tumorous (**c**) human pituitary specimens. Displayed graphically are the means of digestion product isoform contents ± SEM from three replicates for the two types of human pituitary tissue specimens, as indicated.

also contains a large CpG island (−239 to 441) (Figure 6a). Bisulfite sequencing was performed covering the region from 173 to 338, which includes 15 CpG dinucleotide sites. Figure 6b depicts the largely unmethylated status of these individual CpG sites in a normal human specimen. In contrast, tumor 46 reveals evidence of partial methylation in the corresponding region. A microdissected sample (sample B) shows more frequent methylation in FGFR2-negative regions compared with FGFR2-positive staining areas (Figure 6b; see also Figure 7). Figure 6c depicts methylation-specific PCR examination showing lack of methylation of FGFR2 in five of six normal pituitary samples. In contrast, nearly one-half (10 of 22) of human pituitary tumors demonstrated evidence of DNA promoter methylation (Figure 6, c and d). Moreover, in a subset of tumors where DNA and RNA were available from the same samples, we performed parallel RT-PCR and MSP analysis (Figure 6d). This examination revealed that samples with detectable FGFR2 mRNA expression (tumors 44, 47, and 48) were unmethylated. In contrast, tumors with FGFR2 mRNA down-regulation (tumors 42, 43, and 46) showed evidence of promoter DNA methylation (Figure 6d).

Because human pituitary tumor samples can potentially be contaminated with normal, unaffected tissue, we performed MSP analysis on DNA from microdissected specimens that selectively included only tumor cells. In

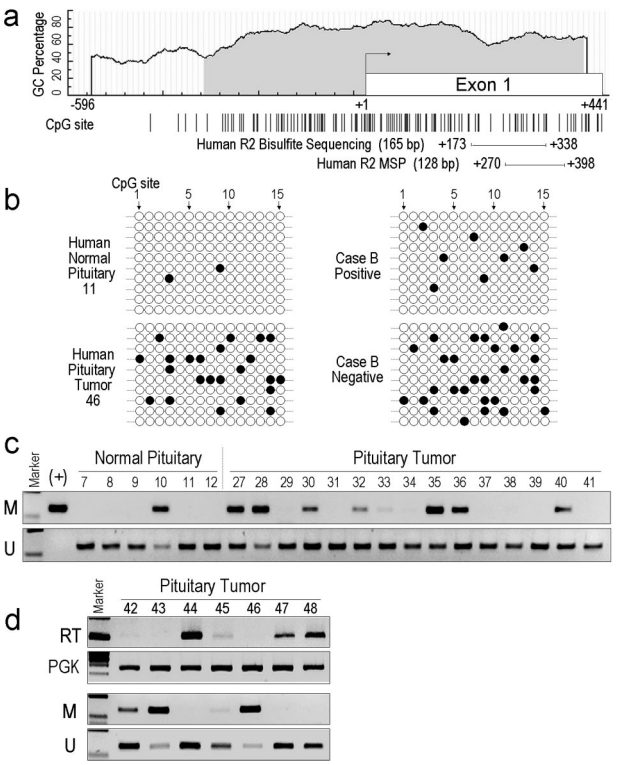

Figure 6. FGFR2 is silenced through selective DNA methylation in human pituitary adenomas. **a:** The human FGFR2 promoter region from −596 to 441 encompassing the 5′-untranslated region and exon 1 contains a large CpG island (−239 to 441). Aberrant CG sites are denoted by vertical bars below the graph. The line indicates the region detected by methylation-specific PCR (MS). Sequence numbering follows GenBank accession NC 000010. **b:** Bisulfite sequencing was performed covering the region from 173 to 338, which includes 15 CpG dinucleotide sites. Results from bisulfite sequencing reveal partial methylation of the gene promoter in neoplastic human pituitary specimens (no. 46). Specimen B (also shown) was resolved after microdissection for FGFR2-positive or -negative immunostaining. Individual methylated CpG sites are indicated by closed circles. Each row represents an individually sequenced clone. **c:** MSP demonstrates changes in methylated (M) and unmethylated (U) DNA levels in normal pituitaries and pituitary tumors obtained from 21 human specimens. Nearly one-half of tumors show evidence of promoter methylation. First lane marked by + denotes a methylated positive control (Universal Methylated DNA). **d:** Both DNA and RNA were extracted from the same seven human pituitary tumor specimens represented by samples numbered 42 to 48, followed by RT-PCR and MSP as indicated. M and U denote methylated and unmethylated, respectively. Note that samples with detectable mRNA expression (specimens 44, 47, and 48) are unmethylated, whereas those showing lack of mRNA abundance (specimens 42, 43, and 46) are methylated.

three independent cases, we found the FGFR2 promoter to be methylated in FGFR2-negative regions (Figure 7). In contrast, tissue from the adjacent normal gland that stained positively for FGFR2 demonstrated lack of detectable promoter methylation (Figure 7).

Discussion

Inactivation of the FGFR2 gene results in profound developmental impact, particularly on endocrine cells including the pituitary gland.[12] Thus far, however, there has been limited information on FGFR2 expression or its possible dysregulation in normal and neoplastic pituitary cells.

Using multiple approaches, we identified the presence of both FGFR2-IIIb and FGFR2-IIIc isoforms in normal mouse and human pituitary cells. Moreover, when expressed in neoplastic pituitary tumor cells, both isoforms were detectable. Pharmacological methylation inhibition, however, resulted in mainly FGFR2-IIIb re-expression with minimal impact on the IIIc isoform. Similar findings of FGFR2-IIIb isoform silencing have been previously noted in prostate cancer.[24] It has been suggested that the putative RNA polymerase II (RNAPII)-pausing MAZ4 element may contribute to changes in the transcription elongation complex that influences alternative splicing decisions yielding these two FGFR2 isoforms.[29] The extent to which such a mechanism is involved in neoplastic-based decisions, however, remains to be determined.

FGFR2-IIIb has been reported to be down-regulated in a subset of transitional cell carcinomas of the bladder,[22,23] and reintroduction of FGFR2-IIIb into T24 bladder cancer cells results in tumor growth inhibition, suggesting that FGFR2 gene inactivation may be implicated in the tumorigenic process rather than a consequence of it. However, unlike in our study, 5′-azacytidine treatment failed to result in re-expression of FGFR2 in bladder tumor cells.[23] There is evidence, at least in osteosarcomas, that the FGFR2 locus on chromosome 10q26 maybe the subject of loss of heterozygosity.[30] However, extensive genome-wide amplification and allelotyping of human pituitary tumors failed to identify such losses at this region.[31] Our studies suggest that the mechanisms leading to FGFR2 down-regulation in pituitary tumors may be distinct with a predominant role for epigenetic contribution.

Another group reported that restoration of FGFR2-IIIb inhibits recruitment of the FGFR substrate 2.[32] However, we and others found that re-expression of FGFR2-IIIb restores FGF7-induced FGFR substrate 2 activation.[25] We also show here that FGF-7 treatment results in diminished pituitary AtT20 cell cycle progression. This was evidenced not only by diminished Rb phosphorylation but also by accumulation of the cyclin-dependent kinase inhibitor p27. The latter finding is of particular interest, given that loss of p27 is a recognized feature associated with human pituitary tumor progression.[33,34] Thus, we believe that our data on FGFR2 down-regulation reported here highlight a potential alternative mechanism contributing to the reduction of p27 in pituitary neoplasia.

An emerging theme from studies of human pituitary tumorigenesis has been the evolving significance of epigenetic control rather than intragenic mutations, loss of heterozygosity, or gene rearrangements.[35] For example, despite its well-recognized impact in genetically deficient mice,[36] the Rb tumor suppressor gene is principally silenced through methylation at a CpG island in human pituitary tumor cells.[37–39] Moreover, no inactivating mutations have been identified within the Rb1 promoter region in pituitary tumors that fail to express the protein.[40] Loss of heterozygosity at 13q, the site of the Rb gene, has been identified in rare pituitary tumors with unmethylated Rb.[40]

Epigenetic silencing has also been shown in other tumor suppressors that are considered important in the pituitary. Mice lacking *p27^{kip1}* have an increased propensity to develop multiorgan neoplasia, including pituitary

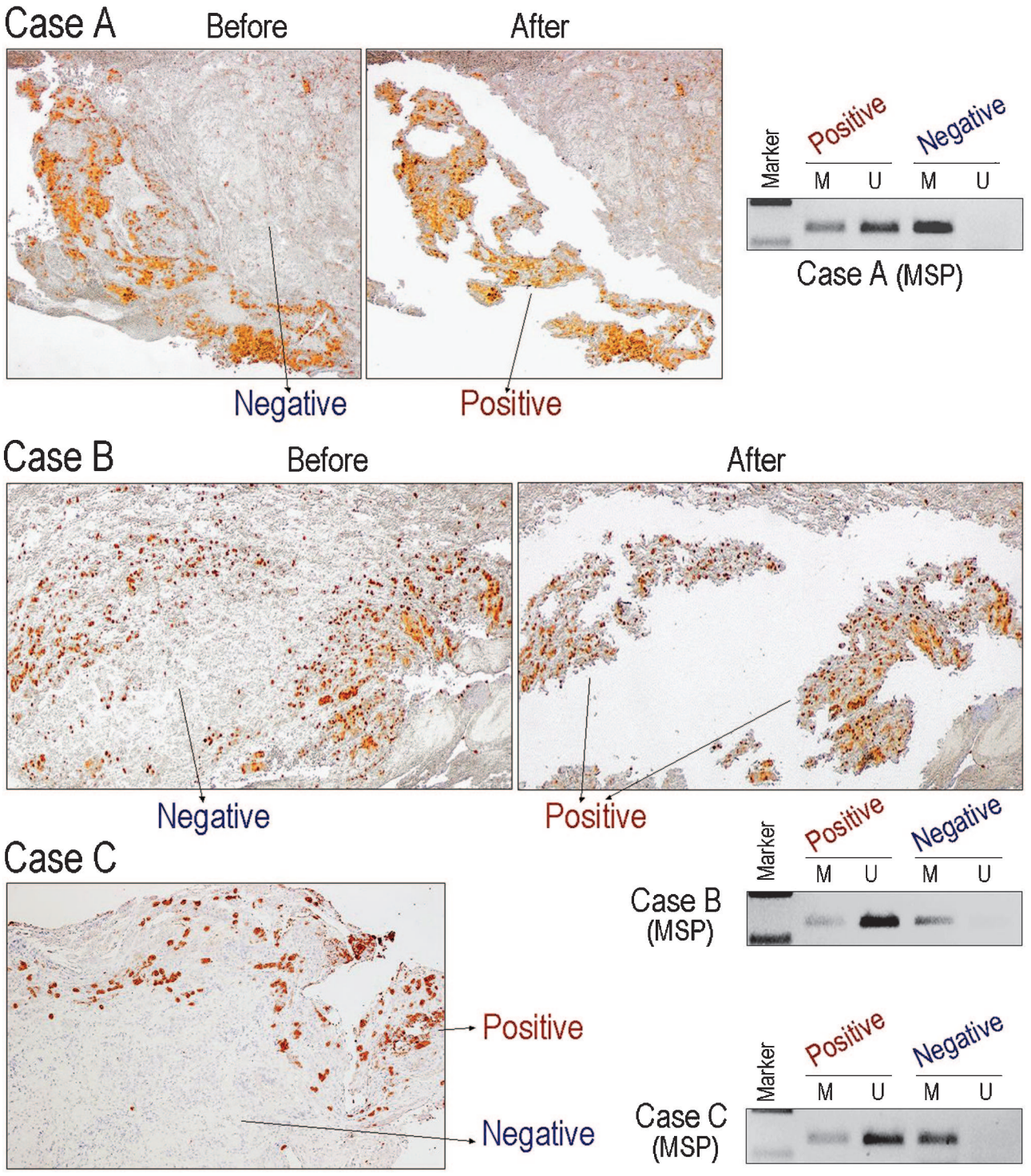

Figure 7. Methylation-specific PCR detection of FGFR2 from microdissected human pituitary tissue. MSP using primers as indicated in Figure 5a was performed on FGFR2-immunostained human pituitary specimens. Shown are three independent cases (**A–C**), each with DNA from corresponding microdissected regions. M and U denote methylation and unmethylation, respectively. Note the lack of appreciable DNA methylation in FGFR2-negative regions.

tumors.[41] Protein levels of this cyclin-dependent kinase inhibitor are reduced in human pituitary adenomas, a feature that correlates with recurrence,[33,34] but the *p27^{kip1}* gene is not mutated; instead, protein levels are diminished through increased ubiquitin-mediated degradation. Likewise, expression of *GADD45γ*, a member of a growth arrest and DNA damage-inducible gene family, is diminished in pituitary adenomas[42] through CpG island promoter methylation.[43] Moreover, MEG3, a human homolog of the mouse maternally imprinted Gtl2 gene, is also down-regulated in human pituitary tumors through 5′ promoter hypermethylation.[44] More recently, a novel

gene on chromosome 22 that confers anti-apoptotic features was isolated from pituitary tumor cells and shown to display some degree of methylation in pituitary adenomas.[45] Another tumor suppressor, Ras-association domain family 1A gene (RASSF1A), recently cloned from the lung tumor locus at 3p21.3 was recently reported to be frequently inactivated by promoter hypermethylation in pituitary tumors.[46]

It has been estimated that approximately 80% of all CpG dinucleotides in the mammalian genome are subject to methylation changes.[47] The remaining unmethylated CpG residues are mostly located in the promoter regions of constitutively active genes referred to as CpG islands. DNA methylation has long been shown to have a transcriptional silencing function with an important role in several tumorigenic states. This is mediated by recruitment of histone deacetylases (HDACs) through the methyl-DNA binding motifs of components of several HDAC-containing complexes.[48] More recently, direct functional links between DNA methylation and histone methylation have been uncovered. Genetic evidence indicates that histone methylation may be a prerequisite for DNA methylation.[49] Our findings on the effect of 5′-azacytidine, classically considered as a DNA-demethylating agent, on histone demethylation support this model. Furthermore, our findings are in agreement with other recent reports supporting the view that DNA and histone methylation may have a reinforcing relationship.[50,51] Moreover, the effects that we observed of TSA treatment on endogenous gene expression and histone methylation further emphasize the potential role of histone modifications on FGFR2 control.

Protein acetylation also plays a crucial role in regulating transcriptional activity. Acetylation complexes (such as CBP/p300) or deacetylation complexes (including HDACs) are typically recruited to DNA-bound transcription factors in response to signaling pathways. Histone hyperacetylation by histone acetyl-transferases are typically associated with transcriptional activation, presumably by remodeling nucleosomal structure into an open conformation that is more accessible to transcription complexes. Conversely, HDAC recruitment is associated with transcriptional repression reversing the chromatin remodeling process. This gene repression can be cell type and promoter specific. However, in the current study, we found little evidence to support the importance of histone acetylation in modulating the FGFR2 gene. These data stand in contrast to those on the FGFR4 gene. In the latter, the 5′ promoter is heavily influenced by HDAC activity, which is recruited through interaction with the zinc finger transcription factor Ikaros.[52] Ikaros represses gene transcription through the HDAC complexes containing mSin3[53] and Mi-2 proteins.[54] Moreover, forced Ikaros expression potently interrupts pharmacologically mediated HDAC inhibition on several promoters, including that for pituitary cell survival signal encoded by Bcl-XL.[55]

Pharmacological interruption of pituitary tumor-derived FGFR4 with the tyrosine kinase inhibitor PD173074 has recently been demonstrated to be of potential value in interrupting neoplastic pituitary growth.[56] Given the remarkable difference between FGFR2 and FGFR4 signaling properties,[57] the current studies underscore the distinct mechanisms by which different members of the FGFR family can be dysregulated in tumorigenesis. They also highlight the complex repertoire of DNA and histone methylation in epigenetic tumor-associated gene silencing.

Acknowledgment

We thank Kelvin So for technical assistance.

References

1. Asa SL, Ezzat S: The cytogenesis and pathogenesis of pituitary adenomas. Endocr Rev 1998, 19:798–827
2. Asa SL, Ezzat S: The pathogenesis of pituitary tumours. Nat Rev Cancer 2002, 2:836–849
3. Treier M, Gleiberman AS, O'Connell SM, Szeto DP, McMahon JA, McMahon AP, Rosenfeld MG: Multistep signaling requirements for pituitary organogenesis in vivo. Genes Dev 1998, 12:1691–1704
4. Paez-Pereda M, Giacomini D, Refojo D, Nagashima AC, Hopfner U, Grubler Y, Chervin A, Goldberg V, Goya R, Hentges ST, Low MJ, Holsboer F, Stalla GK, Arzt E: Involvement of bone morphogenetic protein 4 (BMP-4) in pituitary prolactinoma pathogenesis through a Smad/estrogen receptor crosstalk. Proc Natl Acad Sci USA 2003, 100:1034–1039
5. Itoh N, Ornitz DM: Evolution of the Fgf and Fgfr gene families. Trends Genet 2004, 20:563–569
6. Ornitz DM, Zu J, Colvin JS, McEwen DG, MacArthur CA, Coulier F, Gao G, Goldfarb M: Receptor specificity of the fibroblast growth factor family. J Biol Chem 1996, 271:15292–15297
7. Luo Y, Ye S, Kan M, McKeehan WL: Structural specificity in a FGF7-affinity purified heparin octasaccharide required for formation of a complex with FGF7 and FGFR2IIIb. J Cell Biochem 2006, 97:1241–1258
8. Thisse B, Thisse C, Weston JA: Novel FGF receptor (Z-FGFR4) is dynamically expressed in mesoderm and neurectoderm during early zebrafish embryogenesis. Dev Dyn 1995, 203:377–391
9. Thisse B, Thisse C: Functions and regulations of fibroblast growth factor signaling during embryonic development. Dev Biol 2005, 287:390–402
10. Baraniak AP, Lasda EL, Wagner EJ, Garcia-Blanco MA: A stem structure in fibroblast growth factor receptor 2 transcripts mediates cell-type-specific splicing by approximating intronic control elements. Mol Cell Biol 2003, 23:9327–9337
11. De Moerlooze L, Spencer-Dene B, Revest J, Hajihosseini M, Rosewell I, Dickson C: An important role for the IIIb isoform of fibroblast growth factor receptor 2 (FGFR2) in mesenchymal-epithelial signalling during mouse organogenesis. Development 2000, 127:483–492
12. Celli G, LaRochelle WJ, Mackem S, Sharp R, Merlino G: Soluble dominant-negative receptor uncovers essential roles for fibroblast growth factors in multi-organ induction and patterning. EMBO J 1998, 17:1642–1655
13. Ezzat S, Smyth HS, Ramyar L, Asa SL: Heterogeneous in vivo and in vitro expression of basic fibroblast growth factor by human pituitary adenomas. J Clin Endocrinol Metab 1995, 80:878–884
14. Heaney AP, Horwitz GA, Wang Z, Singson R, Melmed S: Early involvement of estrogen-induced pituitary tumor transforming gene and fibroblast growth factor expression in prolactinoma pathogenesis. Nat Med 1999, 5:1317–1321
15. Asa SL, Ramyar L, Murphy PR, Li AW, Ezzat S: The endogenous fibroblast growth factor-2 antisense gene product regulates pituitary cell growth and hormone production. Mol Endocrinol 2001, 15:589–599
16. Abbass SAA, Asa SL, Ezzat S: Altered expression of fibroblast growth factor receptors in human pituitary adenomas. J Clin Endocrinol Metab 1997, 82:1160–1166
17. Ezzat S, Zheng L, Zhu XF, Wu GE, Asa SL: Targeted expression of a

human pituitary tumor-derived isoform of FGF receptor-4 recapitulates pituitary tumorigenesis. J Clin Invest 2002, 109:69–78
18. Ezzat S, Yu S, Asa SL: Ikaros isoforms in human pituitary tumors: distinct localization, histone acetylation, and activation of the 5′ fibroblast growth factor receptor-4 promoter. Am J Pathol 2003, 163:1177–1184
19. Yu S, Asa SL, Weigel RJ, Ezzat S: Pituitary tumor AP-2alpha recognizes a cryptic promoter in intron 4 of fibroblast growth factor receptor 4. J Biol Chem 2003, 278:19597–19602
20. Ezzat S, Zheng L, Asa SL: Pituitary tumor-derived fibroblast growth factor receptor 4 isoform disrupts neural cell-adhesion molecule/N-cadherin signaling to diminish cell adhesiveness: a mechanism underlying pituitary neoplasia. Mol Endocrinol 2004, 18:2543–2552
21. Fujisawa H, Kurrer M, Reis RM, Yonekawa Y, Kleihues P, Ohgaki H: Acquisition of the glioblastoma phenotype during astrocytoma progression is associated with loss of heterozygosity on 10q25-qter. Am J Pathol 1999, 155:387–394
22. Ricol D, Cappellen D, El Marjou A, Gil-Diez-de-Medina S, Girault JM, Yoshida T, Ferry G, Tucker G, Poupon MF, Chopin D, Thiery JP, Radvanyi F: Tumour suppressive properties of fibroblast growth factor receptor 2-IIIb in human bladder cancer. Oncogene 1999, 18:7234–7243
23. Bernard-Pierrot I, Ricol D, Cassidy A, Graham A, Elvin P, Caillault A, Lair S, Broet P, Thiery JP, Radvanyi F: Inhibition of human bladder tumour cell growth by fibroblast growth factor receptor 2b is independent of its kinase activity: involvement of the carboxy-terminal region of the receptor. Oncogene 2004, 23:9201–9211
24. Naimi B, Latil A, Fournier G, Mangin P, Cussenot O, Berthon P: Down-regulation of (IIIb) and (IIIc) isoforms of fibroblast growth factor receptor 2 (FGFR2) is associated with malignant progression in human prostate. Prostate 2002, 52:245–252
25. Kondo T, Zheng L, Liu W, Kurebayashi J, Asa SL, Ezzat S: Epigenetically-controlled fibroblast growth factor receptor 2-signalling imposes on the RAS/BRAF/MAPK pathway to modulate thyroid cancer progression. Cancer Res, in press.
26. Alexander JM: Tumor suppressor loss in pituitary tumors. Brain Pathol 2001, 11:342–355
27. Asa SL: Tumors of the pituitary gland. Atlas of Tumor Pathology, Third Series, Fascicle 22. Washington, DC, Armed Forces Institute of Pathology, 1998
28. DeLellis RA, Lloyd RV, Heitz PU, Eng C: Tumours of endocrine organs. World Health Organization Classification of Tumours. Lyons, France, IARC, 2004
29. Robson-Dixon ND, Garcia-Blanco MA: MAZ elements alter transcription elongation and silencing of the fibroblast growth factor receptor 2 exon IIIb. J Biol Chem 2004, 279:29075–29084
30. Mendoza S, David H, Gaylord GM, Miller CW: Allelic loss at 10q26 in osteosarcoma in the region of the BUB3 and FGFR2 genes. Cancer Genet Cytogenet 2005, 158:142–147
31. Simpson DJ, Bicknell EJ, Buch HN, Cutty SJ, Clayton RN, Farrell WE: Genome-wide amplification and allelotyping of sporadic pituitary adenomas identify novel regions of genetic loss. Genes Chromosomes Cancer 2003, 37:225–236
32. Zhang Y, Wang H, Toratani S, Sato JD, Kan M, McKeehan WL, Okamoto T: Growth inhibition by keratinocyte growth factor receptor of human salivary adenocarcinoma cells through induction of differentiation and apoptosis. Proc Natl Acad Sci USA 2001, 98:11336–11340
33. Bamberger CM, Fehn M, Bamberger AM, Ludecke DK, Beil FU, Saeger W, Schulte HM: Reduced expression levels of the cell-cycle inhibitor p27Kip1 in human pituitary adenomas. Eur J Endocrinol 1999, 140:250–255
34. Lidhar K, Korbonits M, Jordan S, Khalimova Z, Kaltsas G, Lu X, Clayton RN, Jenkins PJ, Monson JP, Besser GM, Lowe DG, Grossman AB: Low expression of the cell cycle inhibitor p27Kip1 in normal corticotroph cells, corticotroph tumors, and malignant pituitary tumors. J Clin Endocrinol Metab 1999, 84:3823–3830
35. Ezzat S, Asa SL: Mechanisms of disease: the pathogenesis of pituitary tumors. Nat Clin Pract Endocrinol Metab 2006, 2:220–230
36. Jacks T, Fazeli A, Schmitt EM, Bronson RT, Goodell MA, Weinberg RA: Effects of an Rb mutation in the mouse. Nature 1992, 359:295–300
37. Woloschak M, Yu A, Xiao J, Post KD: Abundance and state of phosphorylation of the retinoblastoma gene product in human pituitary tumors. Int J Cancer 1996, 67:16–19
38. Pei L, Melmed S, Scheithauer B, Kovacs K, Benedict WF, Prager D: Frequent loss of heterozygosity at the retinoblastoma susceptibility gene (RB) locus in aggressive pituitary tumors: evidence for a chromosome 13 tumor suppressor gene other than RB. Cancer Res 1995, 55:1613–1616
39. Simpson DJ, Hibberts NA, McNicol AM, Clayton RN, Farrell WE: Loss of pRb expression in pituitary adenomas is associated with methylation of the RB1 CpG island. Cancer Res 2000, 60:1211–1216
40. Bates AS, Farrell WE, Bicknell EJ, McNicol AM, Talbot AJ, Broome JC, Perrett CW, Thakker RV, Clayton RN: Allelic deletion in pituitary adenomas reflects aggressive biological activity and has potential value as a prognostic marker. J Clin Endocrinol Metab 1997, 82:818–824
41. Nakayama K, Ishida N, Shirane M, Inomata A, Inoue T, Shisido N, Horii I, Loh DY: Mice lacking $p27^{Kip1}$ display increased body size, multiple organ hyperplasia, retinal dysplasia, and pituitary tumors. Cell 1996, 85:707–720
42. Zhang X, Sun H, Danila DC, Johnson SR, Zhou Y, Swearingen B, Klibanski A: Loss of expression of GADD45 gamma, a growth inhibitory gene, in human pituitary adenomas: implications for tumorigenesis. J Clin Endocrinol Metab 2002, 87:1262–1267
43. Bahar A, Bicknell JE, Simpson DJ, Clayton RN, Farrell WE: Loss of expression of the growth inhibitory gene GADD45gamma, in human pituitary adenomas, is associated with CpG island methylation. Oncogene 2004, 23:936–944
44. Zhao J, Dahle D, Zhou Y, Zhang X, Klibanski A: Hypermethylation of the promoter region is associated with the loss of MEG3 gene expression in human pituitary tumors. J Clin Endocrinol Metab 2005, 90:2179–2186
45. Bahar A, Simpson DJ, Cutty SJ, Bicknell JE, Hoban PR, Holley S, Mourtada-Maarabouni M, Williams GT, Clayton RN, Farrell WE: Isolation and characterization of a novel pituitary tumor apoptosis gene. Mol Endocrinol 2004, 18:1827–1839
46. Qian ZR, Sano T, Yoshimoto K, Yamada S, Ishizuka A, Mizusawa N, Horiguchi H, Hirokawa M, Asa SL: Inactivation of RASSF1A tumor suppressor gene by aberrant promoter hypermethylation in human pituitary adenomas. Lab Invest 2005, 85:464–473
47. Li E: Chromatin modification and epigenetic reprogramming in mammalian development. Nat Rev Genet 2002, 3:662–673
48. Nan X, Ng HH, Johnson CA, Laherty CD, Turner BM, Eisenman RN, Bird A: Transcriptional repression by the methyl-CpG-binding protein MeCP2 involves a histone deacetylase complex. Nature 1998, 393:386–389
49. Jackson JP, Lindroth AM, Cao X, Jacobsen SE: Control of CpNpG DNA methylation by the KRYPTONITE histone H3 methyltransferase. Nature 2002, 416:556–560
50. Snowden AW, Gregory PD, Case CC, Pabo CO: Gene-specific targeting of H3K9 methylation is sufficient for initiating repression in vivo. Curr Biol 2002, 12:2159–2166
51. McGarvey KM, Fahrner JA, Greene E, Martens J, Jenuwein T, Baylin SB: Silenced tumor suppressor genes reactivated by DNA demethylation do not return to a fully euchromatic chromatin state. Cancer Res 2006, 66:3541–3549
52. Yu S, Asa SL, Ezzat S: Fibroblast growth factor receptor 4 is a target for the zinc-finger transcription factor Ikaros in the pituitary. Mol Endocrinol 2002, 16:1069–1078
53. Koipally J, Renold A, Kim J, Georgopoulos K: Repression by Ikaros and Aiolos is mediated through histone deacetylase complexes. EMBO J 1999, 18:3090–3100
54. Kim J, Sif S, Jones B, Jackson A, Koipally J, Heller E, Winandy S, Viel A, Sawyer A, Ikeda T, Kingston R, Georgopoulos K: Ikaros DNA-binding proteins direct formation of chromatin remodeling complexes in lymphocytes. Immunity 1999, 10:345–355
55. Ezzat S, Zhu X, Loeper S, Fischer S, Asa SL: Tumor-derived Ikaros 6 acetylates the Bcl-XL promoter to up-regulate a survival signal in pituitary cells. Mol Endocrinol 2006, 20:2976–2986
56. Ezzat S, Zheng L, Winer D, Asa SL: Targeting N-cadherin through fibroblast growth factor receptor-4: distinct pathogenetic and therapeutic implications. Mol Endocrinol 2006, 20:2965–2975
57. Ezzat S, Asa SL: FGF receptor signaling at the crossroads of endocrine homeostasis and tumorigenesis. Horm Metab Res 2005, 37:355–360